NKX2-1 regulates cell survival, maturation, and DNA-damage responses as a cofactor of RUNX1 in T-cell acute lymphoblastic leukemia

Linde van Aerschot,[1,2] Sofie Demeyer,[3,4] Kalina Timcheva,[1,2] Elien Heylen,[1,2,5] Paulien Verstraete,[1,2] Dylan De Groote,[1,2] Marino Caruso,[1,2] Lukas Lauwereins,[3,4] Alexandra Veloso,[3,4] Kim R. Kampen,[1,2,6] Daniele Pepe,[1,2] Nancy Boeckx,[7,8] Jonathan Royaert,[1,2] Jelle Verbeeck,[1,2] Heidi Segers,[9,10] Jan Cools,[3,4] Kim De Keersmaecker[1,2#] and David Cabrerizo Granados[1,2#]

[1]Laboratory for Disease Mechanisms in Cancer, Department of Oncology, KU Leuven, Leuven, Belgium; [2]Laboratory for Disease Mechanisms in Cancer, Leuven Cancer Institute (LKI), Leuven, Belgium; [3]Laboratory of Molecular Biology of Leukemia, Department of Human Genetics, KU Leuven, Leuven, Belgium; [4]Laboratory of Molecular Biology of Leukemia, Center for Cancer Biology, VIB, Leuven, Belgium; [5]Centre for Tumour Microenvironment, Barts Cancer Institute, Queen Mary University of London, London, UK; [6]Department of Radiation Oncology (MAASTRO), Maastricht University Medical Center, GROW School for Oncology and Reproduction, Maastricht, the Netherlands; [7]Department of Laboratory Medicine, UZ Leuven, Leuven, Belgium; [8]Laboratory of Experimental Hematology, Department of Oncology, KU Leuven, Leuven, Belgium; [9]Paediatric Haematology and Oncology, University Hospitals Leuven, Leuven, Belgium and [10]Department of Oncology / Pediatric Oncology, KU Leuven, Leuven, Belgium

[#]DCG and KDK contributed equally as senior authors.

Correspondence: D.C. Granados
dcabrerizo-ibis@us.es

K. De Keersmaecker
kim.dekeersmaecker@kuleuven.be

Received: April 8, 2025.
Accepted: December 24, 2025.
Early view: January 8, 2026.

https://doi.org/10.3324/haematol.2025.287966

SUPPLEMENTARY DATA

NKX2-1 regulates cell survival, maturation, and DNA-damage responses as a cofactor of RUNX1 in T-cell acute lymphoblastic leukemia.

This file contains:

- **SUPPLEMENTARY METHODS**
- **SUPPLEMENTARY REFERENCES**
- **SUPPLEMENTARY TABLE S2**
- **SUPPLEMENTARY FIGURES S1-S21**

TABLE S1 is provided as a separate excel file.

Legend TABLE S1: Description of 496 peaks identified by MACS2 in NKX2-1 ChIP-seq analysis.

SUPPLEMENTARY METHODS

Cell culture

RPMI-8402 (ACC 290), DND-41 (ACC 525), SUP-T1 (ACC 140), HPB-ALL (ACC 483), ALL-SIL (ACC 511), LOUCY (ACC 394), PEER (ACC 6), PF-382 (ACC 38), MOLT-4 (ACC 362), MOLT-16 (ACC 29) and HEK-293T (ACC 635) cell lines were obtained from the German Collection of Microorganisms and Cell Cultures GmbH (DSMZ) and Jurkat (TIB-152) from ATCC. T-ALL cells were cultured in RPMI-1640 (Gibco) supplemented with 10% Fetal Calf Serum (FCS) (Gibco). HEK-293T cells were grown in DMEM (Thermo Fisher Scientific) supplemented with 10% fetal bovine serum (Thermo Fisher Scientific, #1017760). OP9-hDLL4 cells (kindly gifted by Tom Taghon) were grown in α-MEM medium (Invitrogen) supplemented with 20% FBS. All cells grew in a humidified cell-culture incubator at 37°C with 5% CO_2, except for OP9-hDLL4 which was grown at 7% CO_2, and were regularly confirmed to be mycoplasma negative.

T-ALL cell line RNA-sequencing data

RNA-seq data from T-ALL cell lines were previously described in Atak *et al*. [1]

Immunoblotting

Cells were lysed in cell lysis buffer (CST, #9803) supplemented with 5 mM Na_3VO_4 and cOmplete protease inhibitor (Roche) and denatured in 1X Laemmli sample buffer (Bio-Rad) containing β-mercaptoethanol (Sigma-Aldrich) at 96°C for 10 min. Proteins were separated on 4-15% Criterion Tris-Glycine eXtended gels (Bio-Rad) and transferred to PVDF membranes. For analyzing histone marks, 12% gels were used (Bio-Rad). After the membranes were incubated with primary and secondary antibodies (**Table 1**), proteins were visualized through chemiluminescence on an Azure C600 (Azure Biosystems). Quantification was performed using the LI-COR Image Studio Lite software using vinculin, histone 3 or Lamin B1 for protein input normalization.

Table 1. Primary and secondary antibodies used for immunoblotting

Target	Catalog number	Company	Target	Catalog number	Company
TTF1/NKX2-1	ab76013	Abcam	H3K27ac	ab4729	Abcam
RUNX1	PA5-19638	Thermo Fisher Scientific	H3K27me3	9733	Cell Signaling Technology
γ–H2AX	9718	Cell Signaling	H3K4me1	39297	Actif Motif

		Technology			
Histone 3	4620	Cell Signaling Technology	H3K4me3	ab8580	Abcam
H3K56ac	MA553741	Invitrogen	H4K20me3	703863	Invitrogen
RPA1	2267	Cell Signaling Technology	CD45	sc-25590	Santa Cruz
CDK6	3136	Cell Signaling Technology	Lamin B1	66095-1-Ig	Proteintech
Vinculin	V9131	Sigma	Tubulin	T5168	Sigma
2ndary anti-Mouse	31432	Thermo Fisher Scientific	2ndary anti-Rabbit	31462	Thermo Fisher Scientific
2ndary anti-Rabbit light chain specific	SA00001-7L	Proteintech			

Quantitative RT-PCR

Total RNA was extracted with RNeasy kit (Qiagen) followed by cDNA synthesis of 500 ng RNA using GoScript reverse transcriptase with random primers (Promega). mRNA expression levels of *NKX2-1* (Fw-AACCAAGCGCATCCAATCTCAAGG; Rv-TGTGCCCAGAGTGAAGTTTGGTCT) and *CDK6* (Fw-TCCCTCCTTTGAAGTGGATG; Rv-GTCACCTGGGGCTAAATGAA) together with *ACTB* (Fw-GTCACCAACTGGGACGACAT; Rv-GAGGCGTACAGGGATAGCAC) as a reference gene were analyzed in triplicates with SYBR Green qRT-PCR (Promega) on a CFX Connect Instrument (BioRad) and quantified using the $\Delta\Delta$Ct method.

Flow cytometry

Immunophenotyping was performed using the antibodies listed in **Table 2**. Proliferation was assessed by cell cycle analysis. Cells were fixed and permeabilized with 70% ethanol, followed by a stain of the DNA by using propidium iodide (PI) with RNAse A. Apoptosis was evaluated by analyzing annexin-V PE (BioLegend, #640947) in binding buffer (10 mM HEPES, 140 mM NaCl, 2.5 mM $CaCl_2$ at pH 7.4) or cleaved caspase 3 (Cell Signaling Technology, #9664) followed by a secondary staining with an Alexa Fluor 488 conjugated anti-rabbit antibody (Thermo Fisher Scientific, #A-11070) in cells fixed and permeabilized with 70% ethanol. Zombie Aqua staining (BioLegend, #423102) was used as a cell viability marker. For viability and drug sensitivity assays, viable cells counts were defined as the proportion of single cells not staining for PI and cell death as single cells staining for PI. For specific cell death, an adaptation of the formula previously described[2] was used: [(% PI positive in the assay well) – (% PI positive in the control well) × 100] ÷ [100 – (% PI positive in the control well)]. O-propargyl puromycin (OPP) labeling was performed according to manufacturer's instructions using the Click-IT OPP Alexa Fluor 647 Protein synthesis Assay kit (Thermo Fisher Scientific, #C10458). Samples were measured on a MACSQuant X flow cytometer (Miltenyi). All data were analyzed using FlowJo software (v10.9).

Table 2. Conjugated antibodies used for immunophenotyping.

Target	Catalog number	Company	Target	Catalog number	Company
CD1a	A07742	Beckman Coulter	CD5	345783	BD Bioscience
CD2	335786	BD Bioscience	CD7	347483	BD Bioscience
sCD3	341101	BD Bioscience	CD34	348053	BD Bioscience
cyCD3	345767	BD Bioscience			

ChIP-sequencing and analysis

For NKX2-1 ChIP-seq: 30 million RPMI-8402 cells were cross-linked for 10 min in 1% formaldehyde, followed by quenching with 0.125M glycine and two washes in ice-cold PBS. Cells were subsequently

sonicated on a Bioruptor NGS (Diagenode) for 12 cycles of 30 s activity – 30 s rest. ChIP was performed using the SimpleChIP Plus Sonication Chromatin IP kit (Cell Signaling), Dynabeads Protein G (Invitrogen) magnetic beads and anti-TTF1/NKX2-1 antibody (Abcam, #ab76013) according to the manufacturer's instructions. DNA was purified using PCR purification columns (Qiagen). KAPA HyperPlus library was constructed and sequenced on the Illumina HiSeq 4000 platform. Obtained single-end 50 bp reads were mapped to the NCBI human reference genome (GRCh38) using Bowtie2 (v2.4.4), filtered using SAMtools (MACQS > 30, v1.18) and deduplicated with Picard (v2.18.23). Next, peaks were called with MACS2 using the NKX2-1$^{-/-}$ clones as background samples and a p-value cut-off of 0.01. Motif analysis was performed using HOMER (v4.11) with default settings.[3] Finally, the peaks were annotated using ChIPseeker (v1.30.3),[4,5] considering the region 3000 bp up- and downstream of the transcription start site (TSS) as the promoter region.

For H3K27ac ChIP-seq: 30 million RPMI-8402 cells were cross-linked for 10 min in 1% formaldehyde, followed by quenching with 0.125M glycine and two washes in ice-cold PBS. For nuclei isolation, cells were resuspended in 1X RSB buffer (10 mM Tris at pH7.4, 10 mM NaCl, 3 mM $MgCl_2$) and left on ice for 10 min to swell. Cells were collected by centrifugation and resuspended in RSBG40 buffer (10 mM Tris at pH7.4, 10 mM NaCl, 3 mM $MgCl_2$, 10% glycerol, 0.5% NP-40) with 1/10 v/v of 10% detergent (3.3% w/v sodium deoxycholate, 6.6% v/v Tween-40). Nuclei were collected by centrifugation and resuspended in L3B+ buffer (10 mM Tris-Cl at pH 8.0, 100 mM NaCl, 1 mM EDTA, 0.5 mM EGTA, 0.1% Na-Deoxycholate, 0.5% N-Lauroylsarcosine, 0.2% SDS). Samples were subsequently sonicated on a Bioruptor NGS (Diagenode) for 10 cycles of 30 s activity – 30 s rest. The chromatin was supplemented with 1% Triton-X100 after fragmentation. H3K27ac antibody (Abcam, #ab4729) was preconjugated to magnetic protein-G beads (Cell Signaling Technology). Chromatin immunoprecipitation was carried out overnight. Tagmentation and library preparation were performed using the Nextera DNA library prep kit (Illumina). DNA was purified using triple sided SPRI bead clean-up (1.2X, 0.6X, 0.9X). (Agencourt AMPure Beads, Beckman Coulter). Sequencing was carried out on an Illumina HiSeq 4000 platform. The raw ChIPmentation sequencing data were first cleaned with fastq-MCF (ea-utils) followed by quality control with fastQC. Reads were mapped to the NCBI human reference genome (GRCh38) using Bowtie2 (v2.4.4), filtered using SAMtools (MACQS > 30, v1.18) and deduplicated with Picard (v2.18.23). Peaks were called with the MACS2 software (v2.2.9.1) and the signals were normalised using DeepTools (v3.5.6).

ATAC sequencing data in RPMI-8402 cells and RUNX1 ChIP-seq in various cell lines data were obtained from the web tool by Oki, S; Ohta, T (2015): ChIP-Atlas. https://chip-atlas.org. [6–8]

Luciferase reporter assays

HEK-293T cells were transfected with a dual-luciferase reporter plasmid containing the identified CDK6 enhancer region chr7:92754552-92755863 (hg38) (**Figure S5A**, VectorBuilder ID: VB250521-1459nsy) as well as with an NKX2-1[9] and/or RUNX1 (Origene code: rc223809) overexpression or control plasmid (pMSCV-GFP) in a 6-well plate using Lipofectamine 3000 (Thermo Fisher Scientific, #L3000001). After 48 h, the cells were lysed, and Firefly and Renilla luciferase expression was measured consecutively using the Dual-Luciferase Reporter Assay System (Promega, E1910) on a Victor X4 multilabel microplate reader (PerkinElmer). Background signal was subtracted from luciferase signals before calculating the relative Firefly/Renilla ratio and normalizing to the control reporter.

Polysome profiling

A 15-55% continuous sucrose gradient was prepared by sequentially layering sucrose solutions of 55%, 45%, 35%, 25%, and 15% containing 20mM HEPES at pH 7.4, 100mM KCl, 10mM $MgCl_2$,

0.1mg/mL Cycloheximide (CHX). Tubes were frozen at -80°C after each layer addition. 20 million cells were treated for 5min with 0.1 µg/µL CHX prior to lysis with lysis buffer containing 5 mM Tris-HCl at pH 7.4, 1.5 mM KCl, 2.5 mM $MgCl_2$, 2 mM Dithiothreitol (DTT), 0.5% Sodium Deoxycholate, 0.5% Triton-X100, 0.1 µg/µL CHX and cOmplete protease inhibitor (Roche). Lysates were cleared by centrifugation (20,000 g, 5 min, 4°C) and gently loaded on top of the thawed sucrose gradients that were subsequently ultracentrifuged (37,000 rpm, 2.5 h, 4°C). Afterwards, the gradients were analyzed for 254 nm absorbance on a BioLogic LP system (BioRad). The polysome profile data was processed and visualized using RStudio (R v4.1.0).

Compounds

Compounds used were Romidepsin (Cayman Chemical), Vorinostat (Cayman Chemical), Etoposide (Selleckchem), Doxorubicin (Cayman Chemical), 6-TG (Tebubio N.V.), Ro5-3335 (MedChemExpress) and AI-10-47 (MedChemExpress). All compounds were dissolved in DMSO.

Alkaline Comet Assay

After drug treatment as specified in the figure legends, cells were mixed with 0.4% low-melting-temperature agarose before being loaded onto slides coated with 1.5% normal agarose. These slides were then lysed overnight at 4°C in a lysis buffer containing 2.5 M NaCl, 10 mM Tris at pH 10.0, 100 mM EDTA, 1% Triton X-100, 1% N-lauroylsarcosine. The slides were further immersed for 20 min in cold electrophoresis buffer containing 0.3 M NaOH, 1 mM EDTA at pH 13.0, followed by electrophoresis (30 mins at 1 V/cm). The slides were then stained with propidium iodide (2.5 µg/mL), visualized under a Nikon Ti2 spinning-disk confocal fluorescence microscope (Tokyo, Japan), and analyzed by OpenComet in Imagej v1.3.1.[10]

Mass spectrometry

Immunoprecipitated samples were eluted, pre-processed and subjected to LC-mass spectrometry at the KU Leuven Proteomics core facility. All spectra were compared against the Human reference proteome database (https://www.uniprot.org/proteomes/UP000005640) using default Spectronaut (v19.2.240905.62635) settings with background level imputation. To identify NKX2-1 binding partners, NKX2-1 co-immunoprecipitated proteins with a fold change above 2 detected in NKX2-$1^{+/+}$ samples against NKX2-$1^{-/-}$ samples, with a q-value below 0.1 and an abundance higher than measured in the IgG-control sample were retained. To analyze the RUNX1 co-immunoprecipitated proteins, only proteins with a fold change above 1.5 and a q-value below 0.05 in the comparison of NKX2-$1^{+/+}$ against NKX2-$1^{-/-}$ samples were retained, with the additional requirement that retained proteins also had to show a fold change above 2 and a q-value below 0.05 compared to the respective IgG samples of their matching genotype. Results were visualized using RStudio (R v4.1.0). The mass spectrometry proteomics data have been deposited to the ProteomeXchange Consortium via the PRIDE partner repository with dataset identifiers PXD057622 and PXD057654.[11]

Patient-derived xenograft (PDX) /OP9-hDLL4 cocultures

2-3 million T-ALL PDX-XB14 cells were seeded onto 6-well plates containing a confluent layer of OP9-hDLL4 cells.[12] After 6 days of PDX/OP9 coculture in α-MEM medium supplemented with 20% FBS, 100 µg/mL Primocin (Invivogen) and 20 ng/mL IL-7 Human Recombinant (200-07, Peprotech) and grown at 7% CO_2, cells were collected for immunoprecipitation or western blotting. For drug treatment experiments, 0.3 million T-ALL PDX cells of each analyzed PDX sample were seeded onto 48-well plates previously seeded with OP9-hDLL4 cells, except for the case of Ro5-3335 where no OP9-hDLL4 were used, in α-MEM medium supplemented with 20% FBS, 100 µg/mL Primocin and 20 ng/mL IL-7 Human Recombinant grown at 7% CO_2.

Statistics

Statistical analyses were performed in GraphPad Prism 10 using the statistical tests indicated in the figure legends. T-tests were two-tailed unpaired. All data presented in the graphs have been checked for normality using the Shapiro-Wilk test. When the data met the assumptions of normality, subsequent analyses were conducted using parametric tests (unpaired t-test). If the data did not meet normality criteria, non-parametric alternatives were applied (Mann–Whitney test). When appropriate, one-way or two-way ANOVA was performed followed by a Tukey's HSD post hoc test or Šidák test. When the data were not normally distributed, a Kruskal-Wallis test followed by a Dunn's post hoc test was applied. The figure legends specify the statistical test used in each figure panel.

SUPPLEMENTARY REFERENCES

1. Kalender Atak Z, Gianfelici V, Hulselmans G, et al. Comprehensive Analysis of Transcriptome Variation Uncovers Known and Novel Driver Events in T-Cell Acute Lymphoblastic Leukemia. PLoS Genet 2013;9(12):e1003997.
2. Epling-Burnette PK, Liu JH, Catlett-Falcone R, et al. Inhibition of STAT3 signaling leads to apoptosis of leukemic large granular lymphocytes and decreased Mcl-1 expression. Journal of Clinical Investigation 2001;107(3):351–362.
3. Heinz S, Benner C, Spann N, et al. Simple Combinations of Lineage-Determining Transcription Factors Prime cis-Regulatory Elements Required for Macrophage and B Cell Identities. Mol Cell 2010;38(4):576–589.
4. Wang Q, Li M, Wu T, et al. Exploring Epigenomic Datasets by ChIPseeker. Curr Protoc 2022;2(10):e585.
5. Yu G, Wang LG, He QY. ChIP seeker: An R/Bioconductor package for ChIP peak annotation, comparison and visualization. Bioinformatics 2015;31(14):2382–2383.
6. Zou Z, Ohta T, Oki S. ChIP-Atlas 3.0: a data-mining suite to explore chromosome architecture together with large-scale regulome data. Nucleic Acids Res 2024;52(W1):W45–W53.
7. Zou Z, Ohta T, Miura F, Oki S. ChIP-Atlas 2021 update: a data-mining suite for exploring epigenomic landscapes by fully integrating ChIP-seq, ATAC-seq and Bisulfite-seq data. Nucleic Acids Res 2022;50(W1):W175–W182.
8. Oki S, Ohta T, Shioi G, et al. ChIP-Atlas: a data-mining suite powered by full integration of public ChIP-seq data. EMBO Rep 2018;19(12):e46255.
9. Heylen E, Verstraete P, Van Aerschot L, et al. Transcription factor NKX2-1 drives serine and glycine synthesis addiction in cancer. Br J Cancer 2023;128(10):1862–1878.
10. Gyori BM, Venkatachalam G, Thiagarajan PS, Hsu D, Clement M-V. OpenComet: An automated tool for comet assay image analysis. Redox Biol 2014;2457–465.
11. Perez-Riverol Y, Bai J, Bandla C, et al. The PRIDE database resources in 2022: A hub for mass spectrometry-based proteomics evidences. Nucleic Acids Res 2022;50(D1):D543–D552.
12. Van De Walle I, De Smet G, Gärtner M, et al. Jagged2 acts as a Delta-like Notch ligand during early hematopoietic cell fate decisions. Blood 2011;117(17):4449–4459.
13. Pölönen P, Di Giacomo D, Seffernick AE, et al. The genomic basis of childhood T-lineage acute lymphoblastic leukaemia. Nature 2024;632(8027):1082–1091.

SUPPLEMENTARY TABLES

TABLE S1 (Description of 496 peaks identified by MACS2 in NKX2-1 ChIP-seq analysis) is provided as a separate excel file.

TABLE S2. Top 25 known motifs identified by HOMER motif analysis ranked on p-value.

HOMER motif analysis on NKX2-1 ChIP-seq from NKX2-1 RPMI-8402 model

RANK	Motif	Name	% of targets	% of background	p-value
1		Fli1(ETS)/CD8-FLI-ChIP-Seq(GSE20898)/Homer	34.27%	15.09%	1e-25
2		RUNX2(Runt)/PCa-RUNX2-ChIP-Seq(GSE33889)/Homer	29.23%	11.90%	1e-24
3		RUNX(Runt)/HPC7-Runx1-ChIP-Seq(GSE22178)/Homer	25.40%	9.50%	1e-23
4		Etv2(ETS)/ES-ER71-ChIP-Seq(GSE59402)/Homer	30.65%	13.27%	1e-23
5		RUNX-AML(Runt)/CD4+-PolII-ChIP-Seq(Barski_et_al.)/Homer	25.60%	10.00%	1e-22
6		RUNX1(Runt)/Jurkat-RUNX1-ChIP-Seq(GSE29180)/Homer	31.85%	14.46%	1e-22
7		Elk4(ETS)/Hela-Elk4-ChIP-Seq(GSE31477)/Homer	19.76%	6.70%	1e-21
8		Elk1(ETS)/Hela-Elk1-ChIP-Seq(GSE31477)/Homer	19.35%	6.60%	1e-20
9		Nkx2.2(Homeobox)/NPC-Nkx2.2-ChIP-Seq(GSE61673)/Homer	50.20%	30.53%	1e-19
10		ELF1(ETS)/Jurkat-ELF1-ChIP-Seq(SRA014231)/Homer	17.94%	6.14%	1e-18
11		Nkx2.5(Homeobox)/HL1-Nkx2.5.biotin-ChIP-Seq(GSE21529)/Homer	52.02%	32.97%	1e-17
12		EWS:ERG-fusion(ETS)/CADO_ES1-EWS:ERG-ChIP-Seq(SRA014231)/Homer	25.60%	11.45%	1e-17
13		GABPA(ETS)/Jurkat-GABPa-ChIP-Seq(GSE17954)/Homer	25.60%	11.62%	1e-17
14		ETS(ETS)/Promoter/Homer	13.10%	3.82%	1e-16
15		ETV1(ETS)/GIST48-ETV1-ChIP-Seq(GSE22441)/Homer	34.27%	18.24%	1e-16
16		ETV4(ETS)/HepG2-ETV4-ChIP-Seq(ENCODE)/Homer	28.83%	14.13%	1e-16
17		STAT5(Stat)/mCD4+-Stat5-ChIP-Seq(GSE12346)/Homer	15.12%	5.18%	1e-15
18		EWS:FLI1-fusion(ETS)/SK_N_MC-EWS:FLI1-ChIP-Seq(SRA014231)/Homer	19.35%	7.81%	1e-15
19		ETS1(ETS)/Jurkat-ETS1-ChIP-Seq(GSE17954)/Homer	28.43%	14.21%	1e-15

20		ETS:RUNX(ETS,Runt)/Jurkat-RUNX1-ChIP-Seq(GSE17954)/Homer	6.45%	1.16%	1e-13
21		ERG(ETS)/VCaP-ERG-ChIP-Seq(GSE14097)/Homer	37.50%	22.36%	1e-13
22		Bapx1(Homeobox)/VertebralCol-Bapx1-ChIP-Seq(GSE36672)/Homer	51.21%	34.59%	1e-13
23		Nkx2.1(Homeobox)/LungAC-Nkx2.1-ChIP-Seq(GSE43252)/Homer	56.45%	40.72%	1e-11
24		Ets1-distal(ETS)/CD4+-PolII-ChIP-Seq(Barski_et_al.)/Homer	11.29%	3.86%	1e-11
25		ZNF189(Zf)/HEK293-ZNF189.GFP-ChIP-Seq(GSE58341)/Homer	23.19%	12.11%	1e-11

SUPPLEMENTARY FIGURES

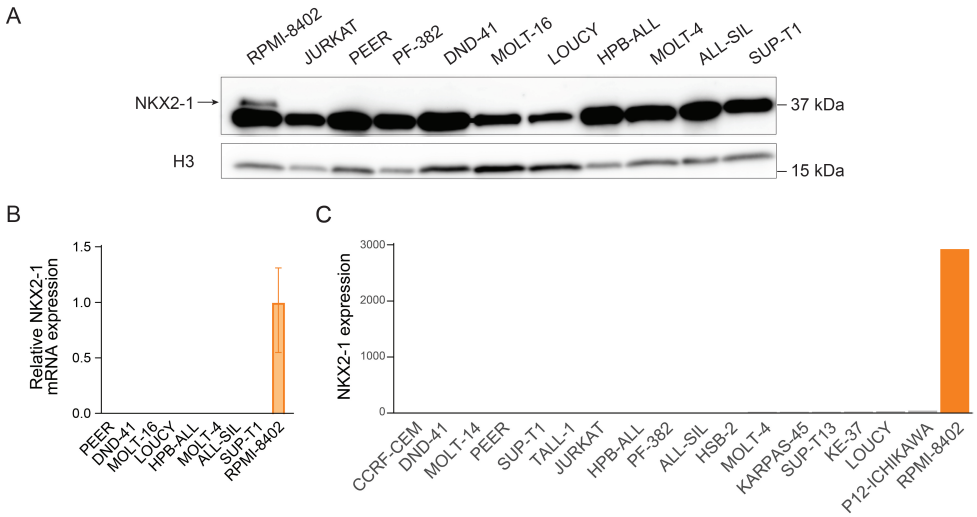

Figure S1. The RPMI-8402 cell line is the only analyzed human T-ALL cell line with endogenous NKX2-1 expression (A) Immunoblot for NKX2-1 in a panel of human T-ALL cell lines. The signal detected at 37 kDa in all cell lines corresponds to a nonspecific band detected by the NKX2-1 antibody. The NKX2-1 specific signal is indicated with an arrow. Histone 3 (H3) detection served as loading control. **(B)** Relative NKX2-1 mRNA expression in RPMI-8402 and other human T-ALL cell lines by RT-qPCR. **(C)** NKX2-1 mRNA expression in RPMI-8402 and 17 other human T-ALL cell lines from Atak *et al*. [1]

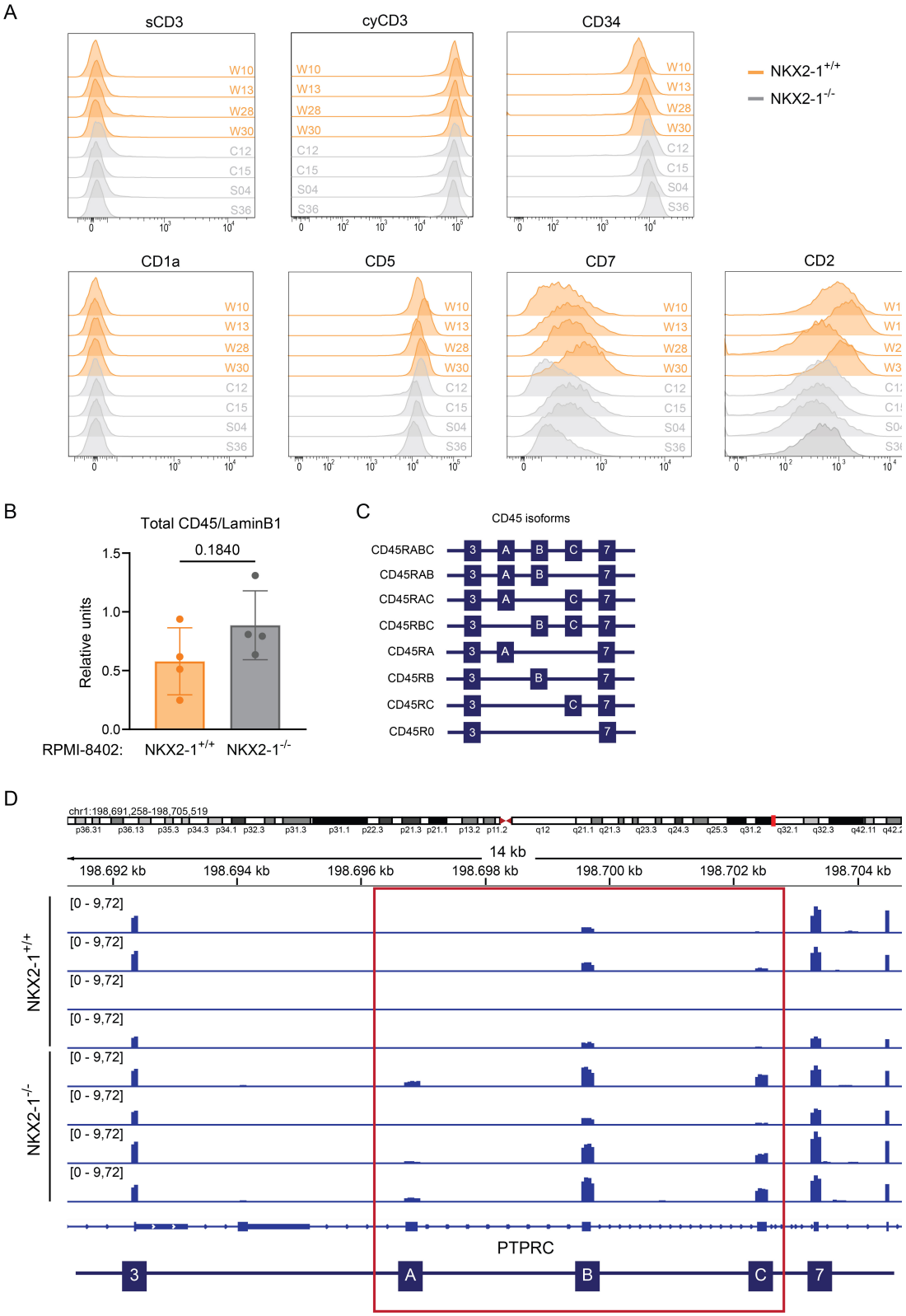

Figure S2. Immunophenotyping and CD45 isoform expression in NKX2-1$^{+/+}$ and NKX2-1$^{-/-}$ RPMI-8402 clones. **(A)** Histograms show flow cytometry signal per clone for each indicated marker. **(B)** Quantification of total CD45 protein expression by western blotting in NKX2-1$^{+/+}$ and NKX2-1$^{-/-}$ RPMI-8402 clones. Data are represented as mean ± SD. Individual dots represent 4 biologically independent clones per genotype. p-values were calculated using an unpaired two-tailed t-test. Western blot is shown in Figure 1D. **(C)** Scheme of PTPRC (CD45) exon-intron structure of the alternatively spliced region in PTPRC. **(D)** Normalized RNA-seq reads at the *PTPRC* locus in RPMI-8402 NKX2-1$^{+/+}$ and NKX2-1$^{-/-}$ clones in IGV. Exons A, B and C of *PTPRC* that exhibit differential splicing are shown at the bottom.

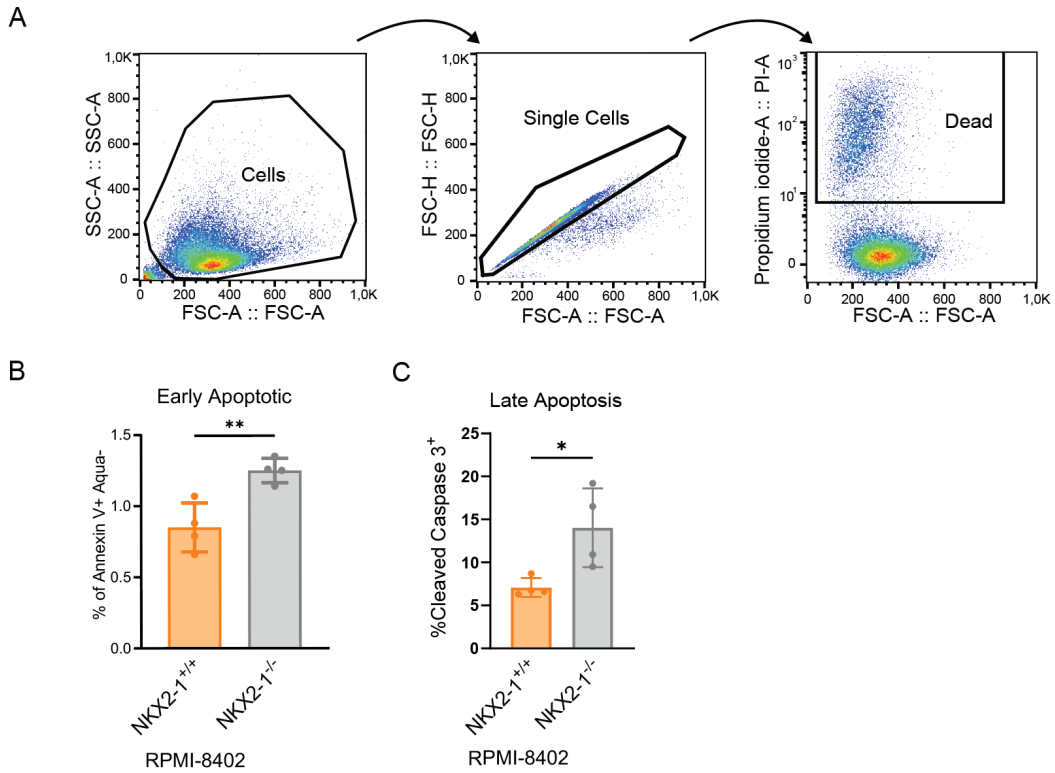

Figure S3. NKX2-1 decreases apoptosis in RPMI-8402 model. (A) Gating strategy for cell death using Propidium Iodide (PI) by flow cytometry. **(B)** Flow cytometry based quantification of Annexin V-positive/Zombie Aqua-negative early apoptotic cells in NKX2-1 $^{+/+}$ and NKX2-1$^{-/-}$ RPMI-8402 clones at day 5. Data represented as mean ± SD, statistics calculated by unpaired two-tailed t-test. **(C)** Flow cytometry based quantification of cleaved caspase 3-positive late apoptotic cells in NKX2-1 $^{+/+}$ and NKX2-1$^{-/-}$ RPMI-8402 clones at day 5. Data are represented as mean ± SD. Individual dots represent 4 biologically independent clones per genotype. p-values were calculated using an unpaired two-tailed t-test. *p-value < 0.05; **p-value < 0.01.

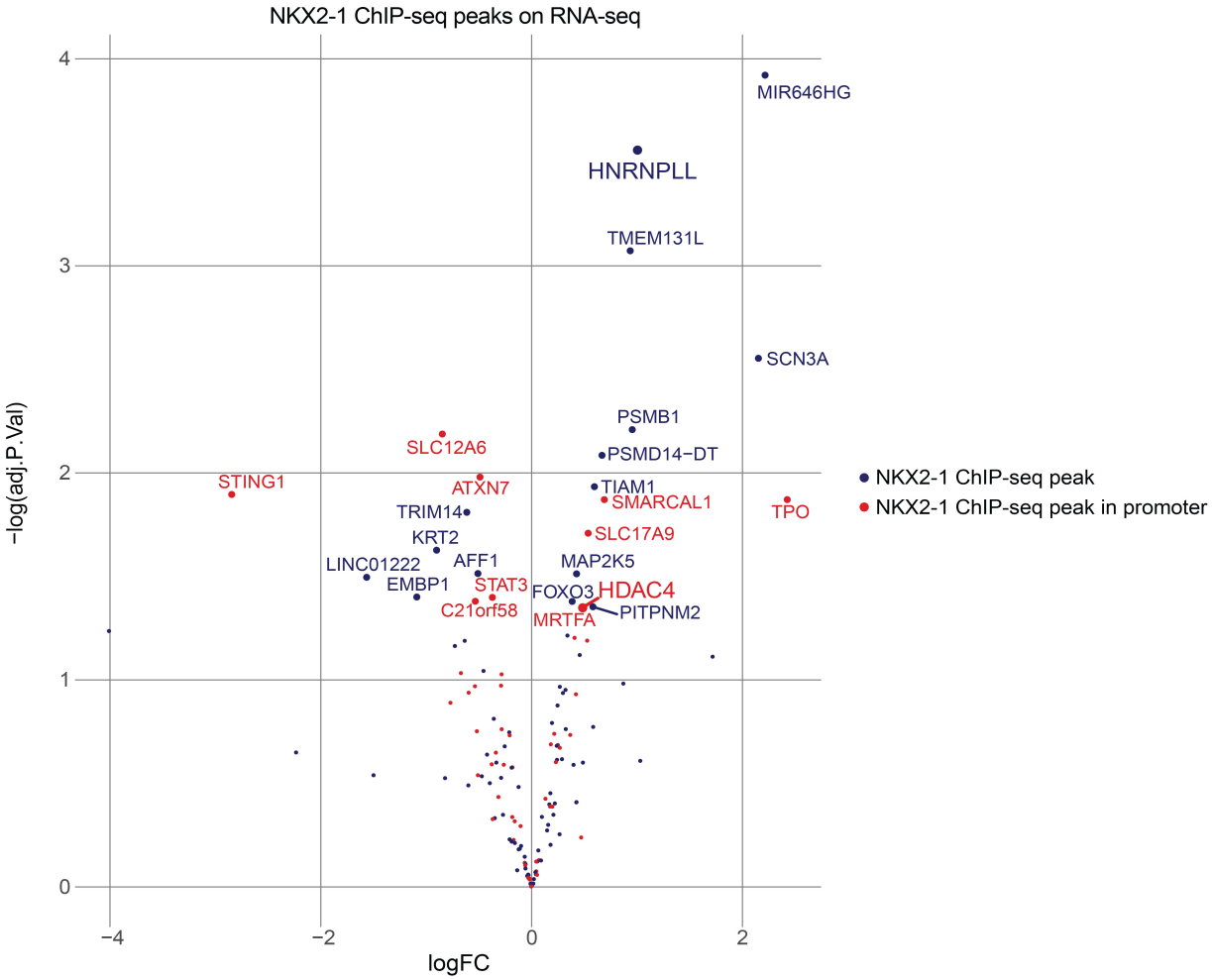

Figure S4. Overlap of RNA-seq and ChIP-seq data obtained from NKX2-1 RPMI-8402 model. Volcano plot showing RNA-seq based expression of genes in NKX2-1$^{+/+}$ versus NKX2-1$^{-/-}$ RPMI-8402 clones that have adjacent peaks in the NKX2-1 ChIP-seq experiment on RPMI-8402 cells. Genes with a significant RNA-seq expression change (–log(adj.P.Val) > 1.3) are labelled with their gene name. Red dots refer to genes with ChIP-seq signal in their promoter region, blue dots are genes with exonic, intronic, 3'UTR or distal intergenic ChIP-seq signal.

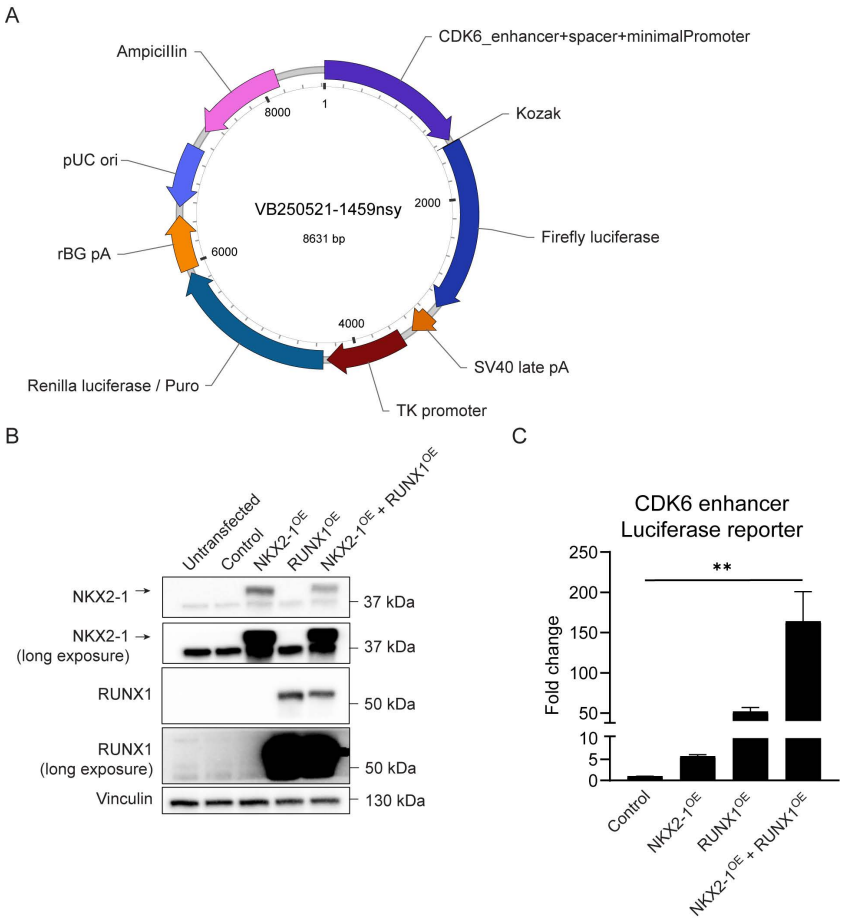

Figure S5. NKX2-1 and RUNX1 synergistically regulate CDK6 enhancer activity. (A) Dual-luciferase plasmid containing the CDK6 enhancer region. **(B)** Western blot analysis of NKX2-1 and RUNX1 expression in HEK-293T cells transfected with CDK6 enhancer luciferase plasmid and co-transfected with empty vector control (pMSCV-GFP), NKX2-1-overpression and/or RUNX1-overexpression plasmids. The NKX2-1 specific signal is indicated with an arrow. Vinculin detection served as loading control. **(C)** Results from dual-luciferase reporter assays in HEK-293T cells. The ratio of Firefly luciferase signal (controlled by CDK6 enhancer followed by minimal promoter) over Renilla luciferase signal (under constitutive TK promoter) serves as a measurement of CDK6 enhancer activity. The graph shows combined data from two independent experiments. Error bars indicate SD. Statistics calculated by Kruskal-Wallis followed by a Dunn's post hoc test: **p-value < 0.01

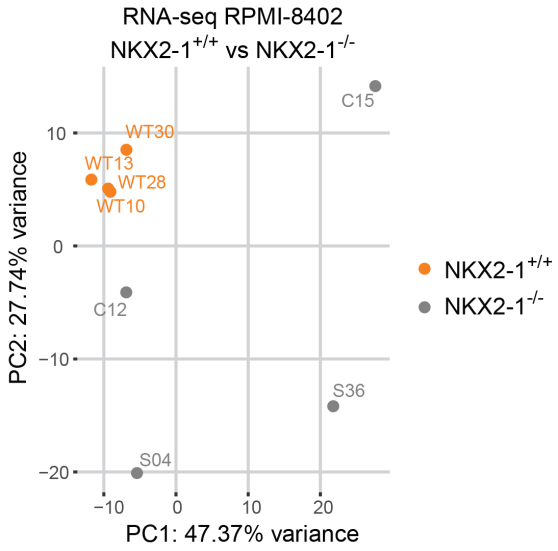

Figure S6. PCA plot showing the variation among the RNA-sequencing samples based on normalized expression data from NKX2-1$^{+/+}$ and NKX2-1$^{-/-}$ RPMI-8402 clones.

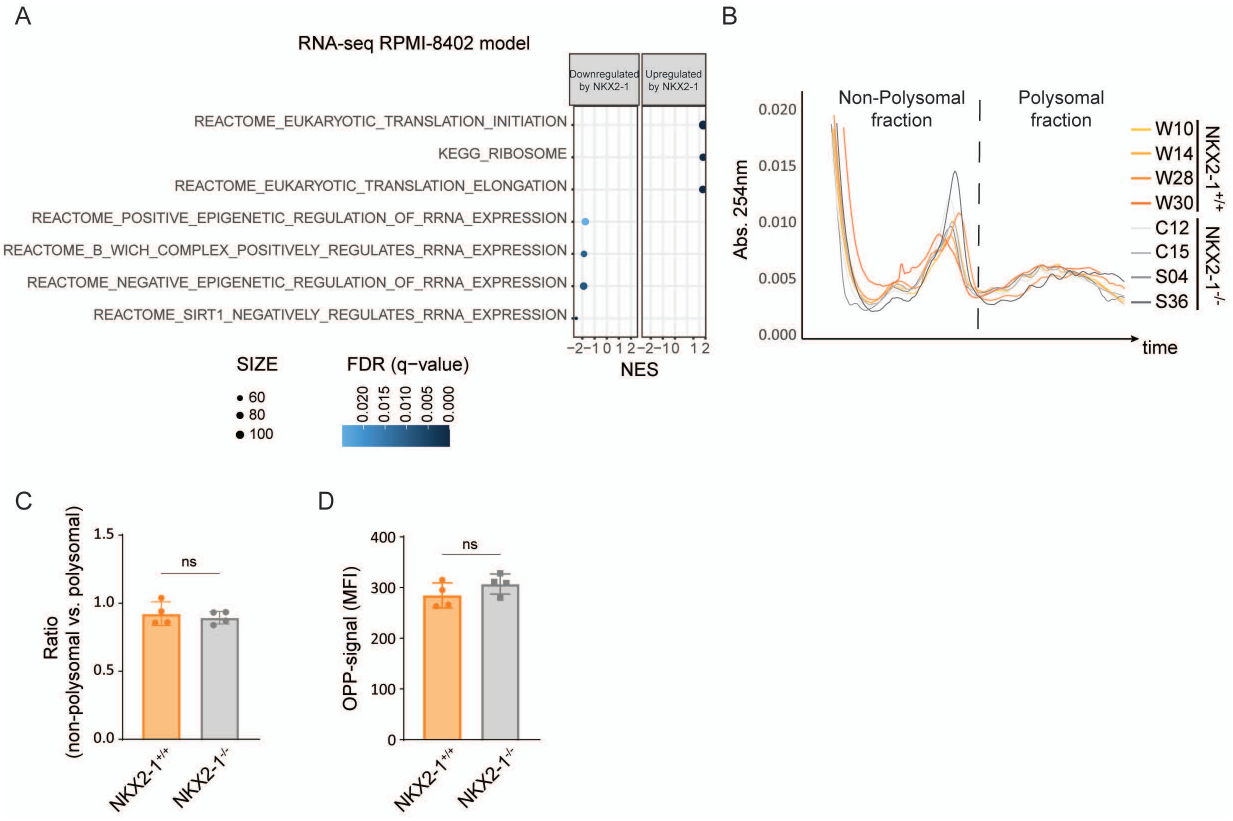

Figure S7. Ribosomal and translational characterization shows no major differences between NKX2-1$^{+/+}$ and NKX2-1$^{-/-}$ clones. (A) Dot plot showing enriched gene sets linked to ribosomes identified in the GSEA of differentially expressed RNA-seq genes in NKX2-1 RPMI-8402 clones. **(B)** Polysome profiles of NKX2-1$^{+/+}$ and NKX2-1$^{-/-}$ clones representing the 254 nm absorbance measured over time. The non-polysomal and polysomal fractions are delimited by the dotted line. **(C)** Ratio between area under the curve of the non-polysomal vs. polysomal fraction in NKX2-1$^{+/+}$ and NKX2-1$^{-/-}$ clones. **(D)** Mean Fluorescent Intensity (MFI) of OPP-positive cells measured by flow cytometry in NKX2-1$^{+/+}$ and NKX2-1$^{-/-}$ clones after OPP treatment for 60 min. Data in panel C and D are represented as mean ± SD. Individual dots represent 4 biologically independent clones per genotype. p-values were calculated using an unpaired two-tailed t-test. Individual dots represent the 4 biologically independent clones per genotype.

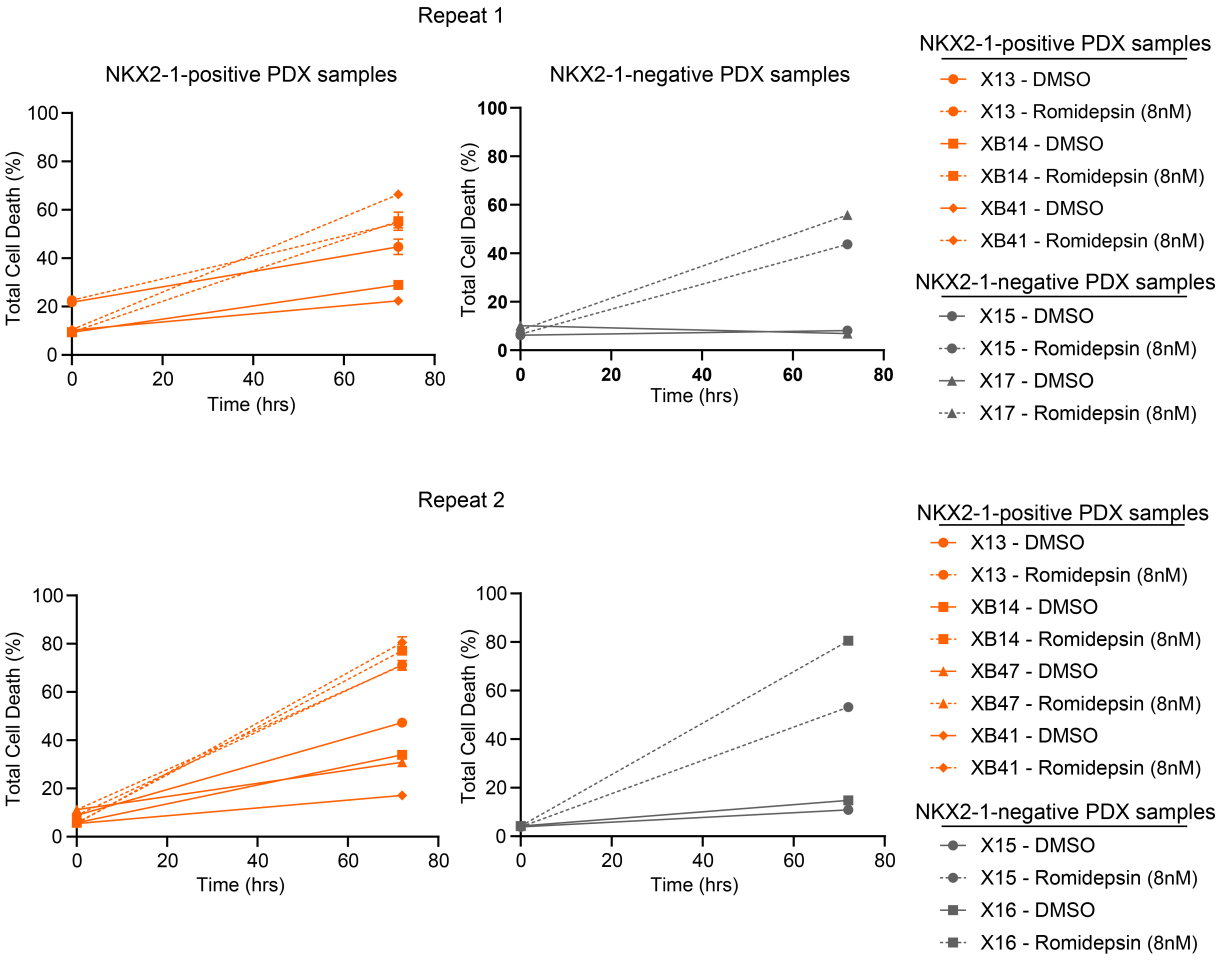

Figure S8. Cell death induced in PDX samples treated with Romidepsin. Total cell death of NKX2-1-positive and NKX2-1-negative PDX samples after Romidepsin treatment for 72 hours. Percentages of dead cells were determined as PI-positive staining cells in flow cytometry.

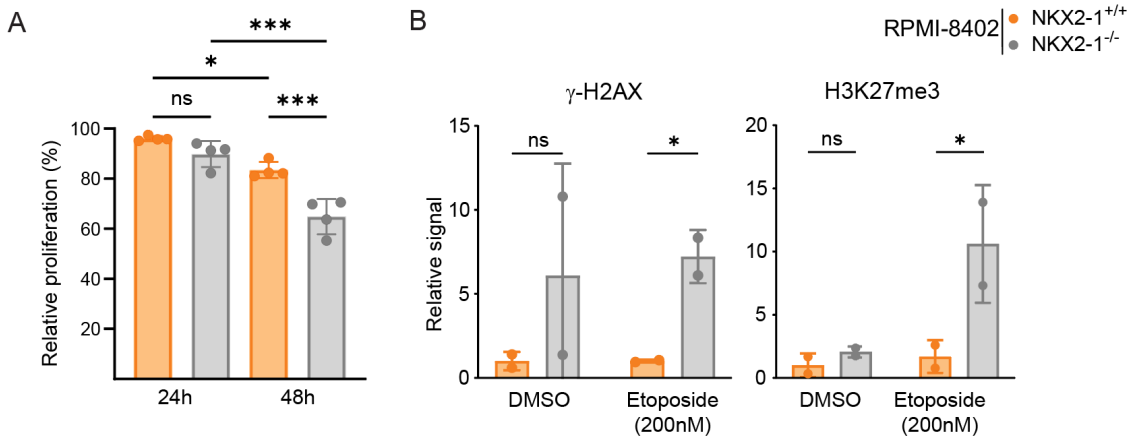

Figure S9. Etoposide effect on NKX2-1 RPMI-8402 model. (A) Relative viability of NKX2-1$^{+/+}$ and NKX2-1$^{-/-}$ RPMI-8402 clones after treatment with Etoposide for 24 and 48 h. Data are normalized to Day 0 and to the DMSO vehicle condition. Data represented as mean ± SD, statistics calculated by an ordinary one-way ANOVA followed by a Tukey's HSD post hoc test. **(B)** Quantification of γ-H2AX (left) and H3K27me3 (right) protein expression by western blotting from two independent experiments combining 4 biologically independent clones per genotype (blots shown in Figure 4C).

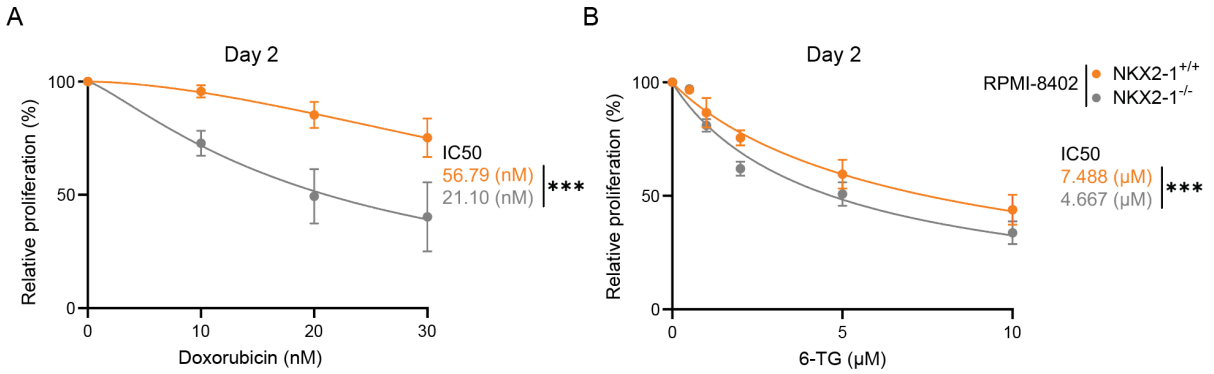

Figure S10. DNA-damaging agents dose response curves for NKX2-1 RPMI-8402 model. Dose-response curves of NKX2-1$^{+/+}$ and NKX2-1$^{-/-}$ RPMI-8402 clones treated for 48 h with Doxorubicin (left) or 6-TG (thioguanine) (right). Data points represent mean ± SD of relative proliferation, normalized to Day 0 and DMSO condition. Least-squares regression fits to the mean are shown (solid lines), and IC50 values were determined for each drug and condition. Statistics were calculated by an extra sum-of-squares F-test. ***p-value < 0.001.

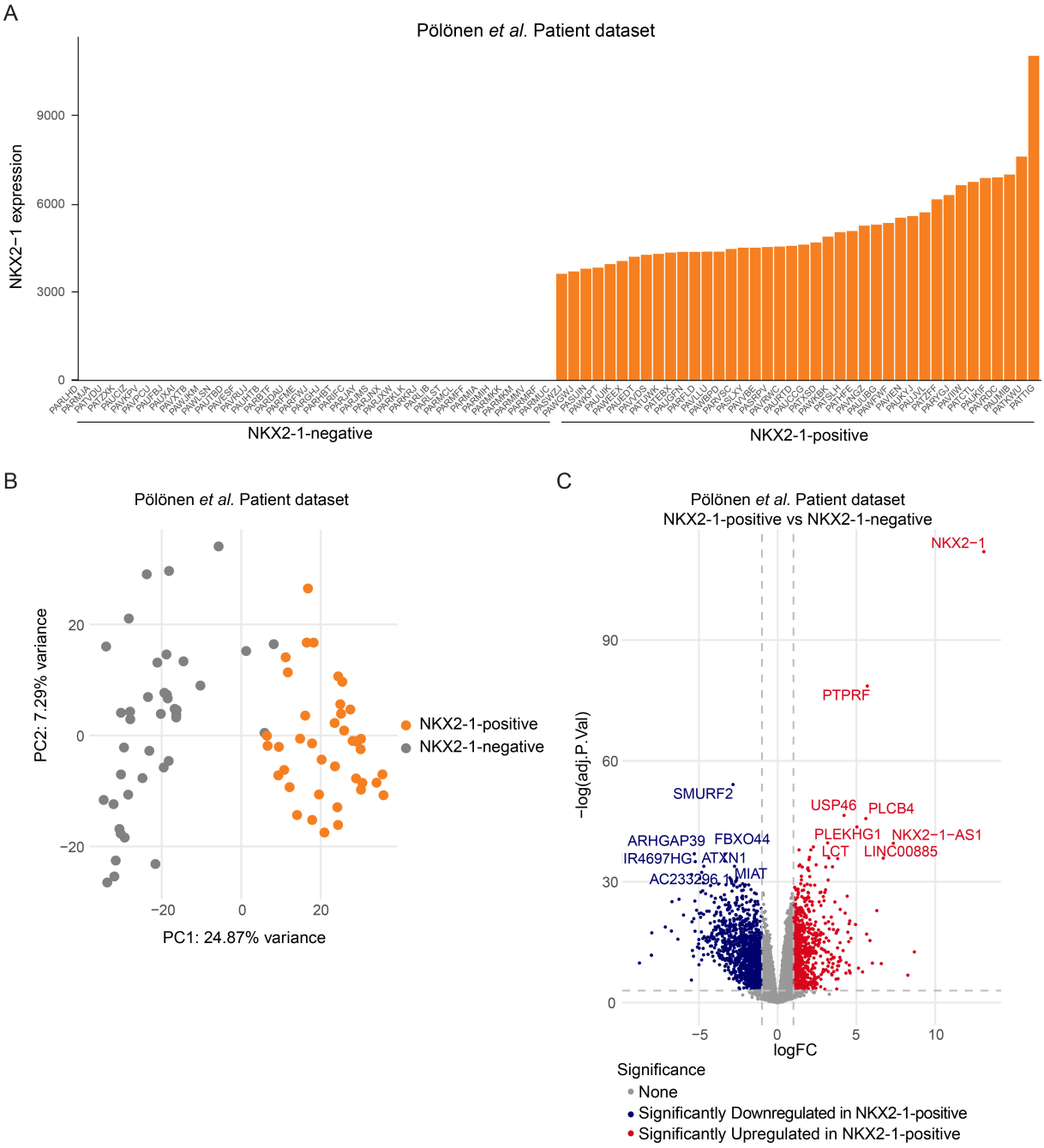

Figure S11. Description of RNA-seq T-ALL Patient dataset of Pölönen *et al.* [13] **(A)** NKX2-1 mRNA expression in 40 NKX2-1-negative TAL1 and 40 NKX2-1-positive T-ALL samples. **(B)** PCA plot showing the variation among the RNA-sequencing samples based on normalized expression data on NKX2-1-negative (grey) and NKX2-1-positive (orange) T-ALL samples. **(C)** Volcano plot showing differentially expressed genes between NKX2-1-positive and NKX2-1-negative T-ALL samples. The grey-dotted lines indicate the cut-off values for significance (adj.P.Val<0.05) and fold change (FC>2).

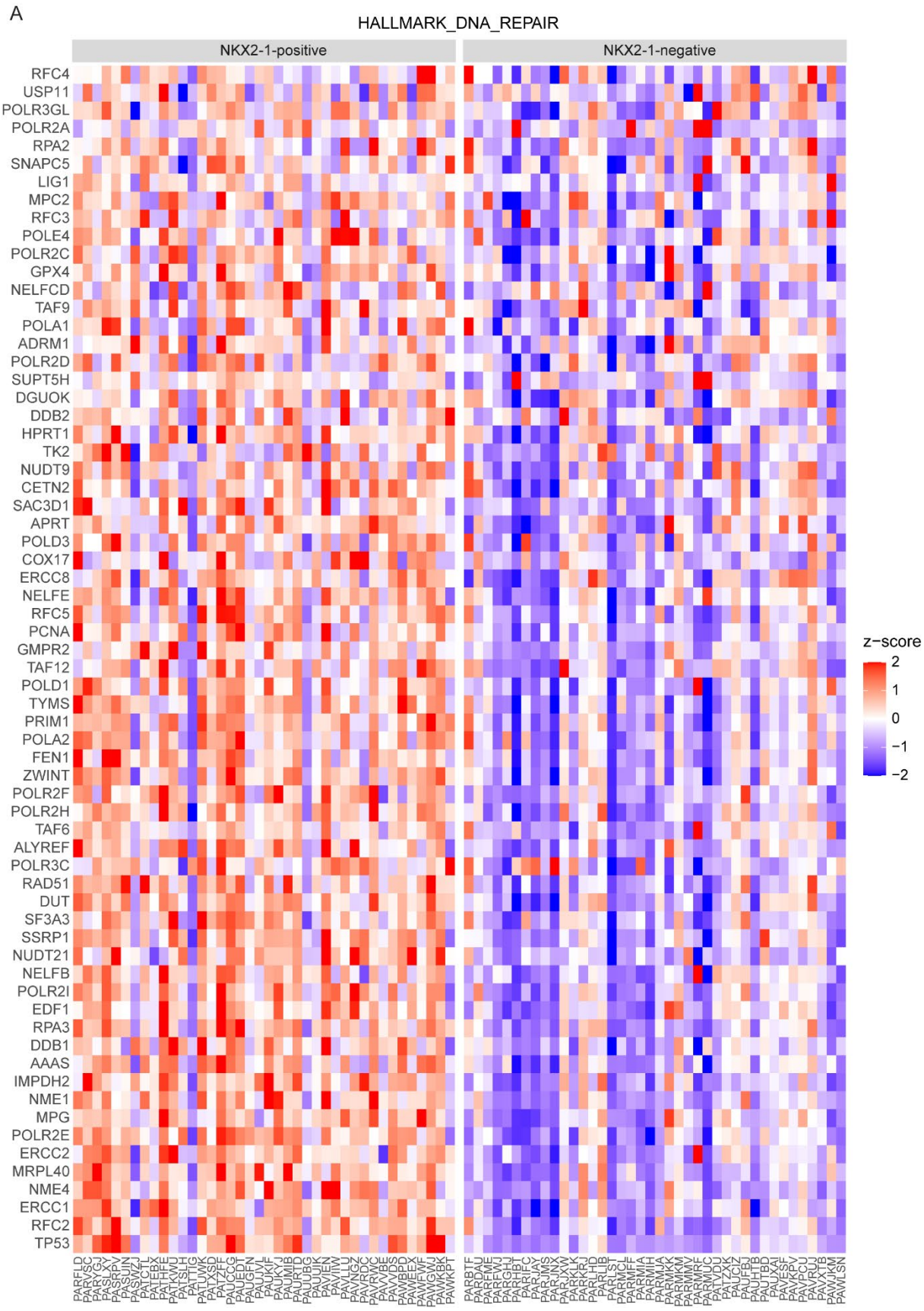
A
HALLMARK_DNA_REPAIR
NKX2-1-positive
NKX2-1-negative
RFC4
USP11
POLR3GL
POLR2A
RPA2
SNAPC5
LIG1
MPC2
RFC3
POLE4
POLR2C
GPX4
NELFCD
TAF9
POLA1
ADRM1
POLR2D
SUPT5H
DGUOK
DDB2
HPRT1
TK2
NUDT9
CETN2
SAC3D1
APRT
POLD3
COX17
ERCC8
NELFE
RFC5
PCNA
GMPR2
TAF12
POLD1
TYMS
PRIM1
POLA2
FEN1
ZWINT
POLR2F
POLR2H
TAF6
ALYREF
POLR3C
RAD51
DUT
SF3A3
SSRP1
NUDT21
NELFB
POLR2I
EDF1
RPA3
DDB1
AAAS
IMPDH2
NME1
MPG
POLR2E
ERCC2
MRPL40
NME4
ERCC1
RFC2
TP53
z−score
2
1
0
−1
−2

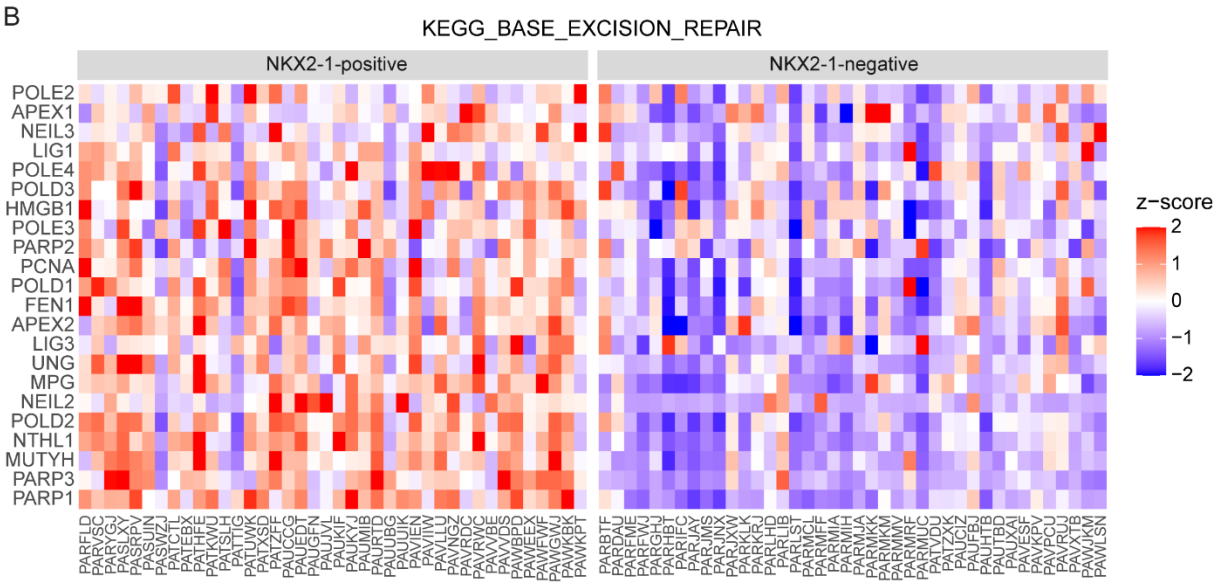

Figure S12. Heatmaps of DNA damage repair related GSEA pathways from Pölönen *et al*. (A-B) Heatmap showing expression of the leading-edge genes in NKX2-1 positive and NKX2-1 negative T-ALL samples of genes in the HALLMARK pathway "DNA_REPAIR" (A) and KEGG pathway "BASE_EXCISION_REPAIR" (B). Expression is shown as mean z-score.

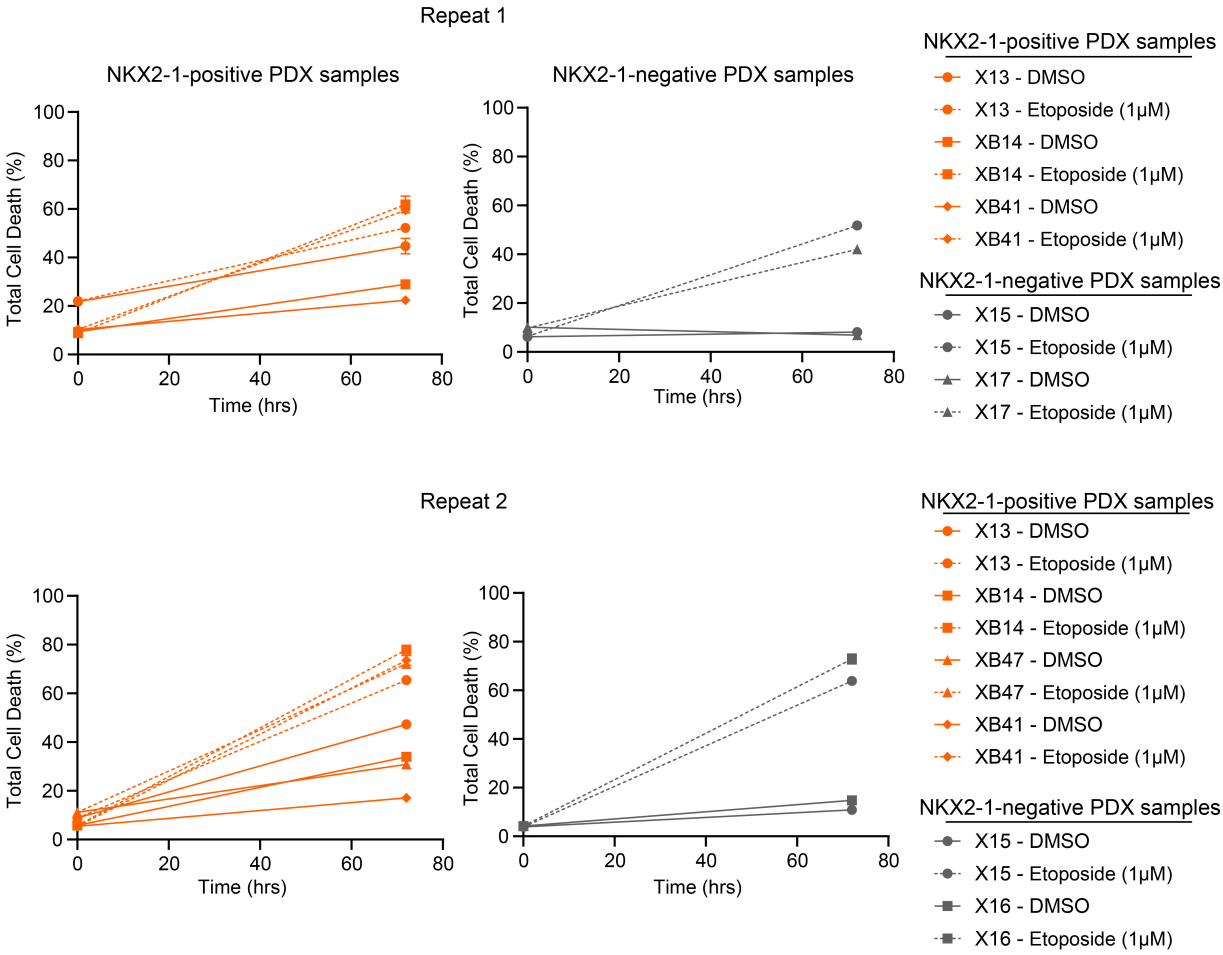

Figure S13. Cell death induced in PDX samples treated with Etoposide. Total cell death of NKX2-1 positive and NKX2-1 negative PDX samples after Etoposide treatment for 72 h. Percentages of dead cells were determined as PI-positive staining cells in flow cytometry.

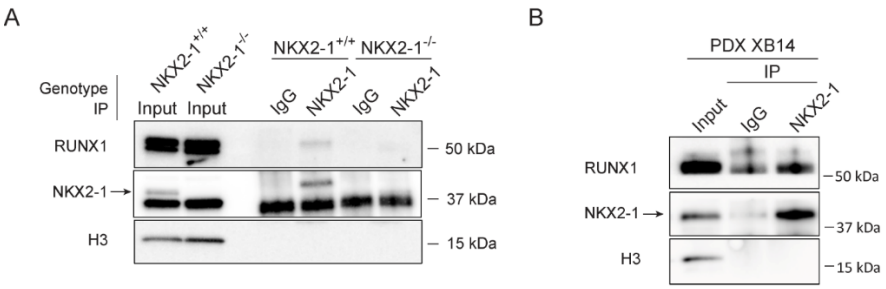

Figure S14. NKX2-1 co-immunoprecipitates with RUNX1 in T-ALL models. (A-B) Immunoblot for RUNX1, NKX2-1 and histone 3 (H3) of input, IgG control and NKX2-1 immunoprecipitated samples of NKX2-1$^{+/+}$ or NKX2-1$^{-/-}$ mixed RPMI-8402 clones (A) or NKX2-1-positive PDX XB14 (B).

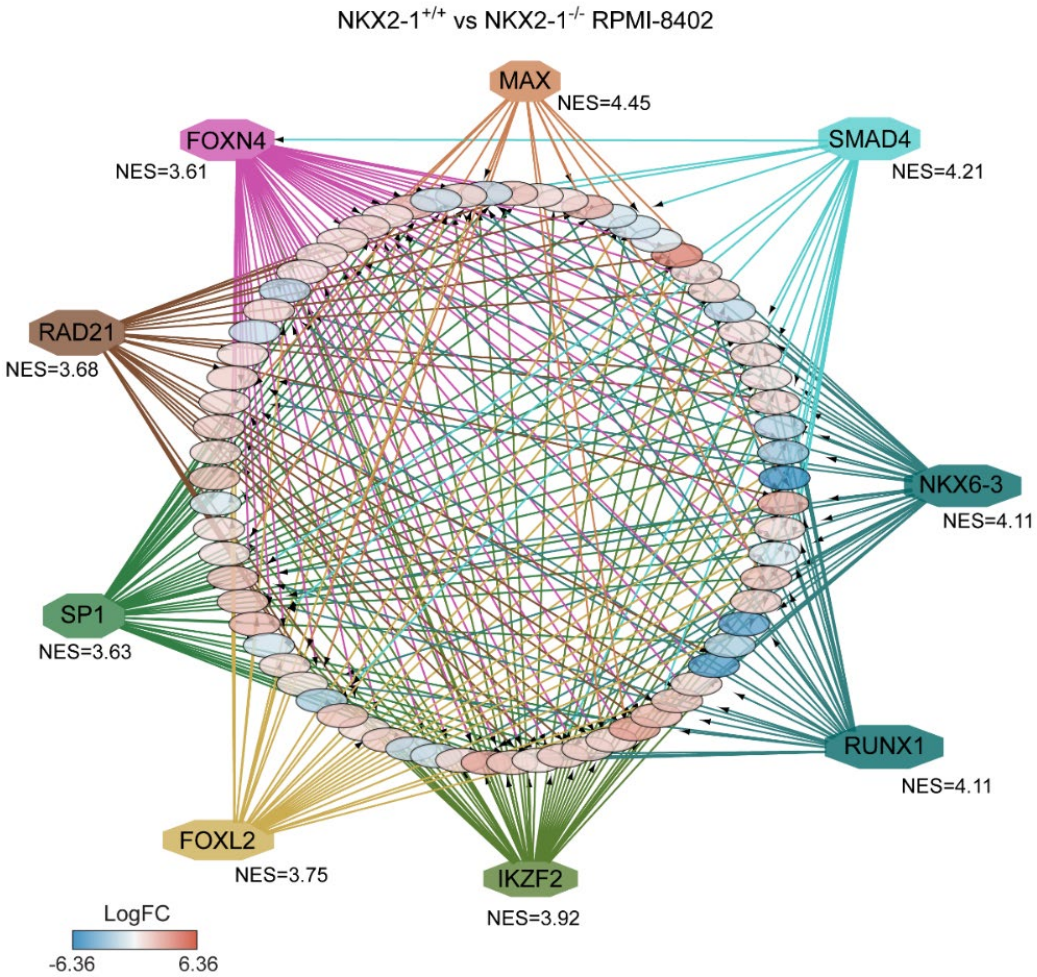

Figure S15. Network representation of transcriptionally regulated genes in RPMI-8402 model. iRegulon analysis on significantly differentially expressed genes (DEGs) in NKX2-1$^{+/+}$ clones compared to NKX2-1$^{-/-}$ clones. Representative transcription factors from 8 top scoring predicted clusters are indicated in the outside octagons. NES values for each cluster code are shown from each transcription factor. DEGs are colored according to their logFC.

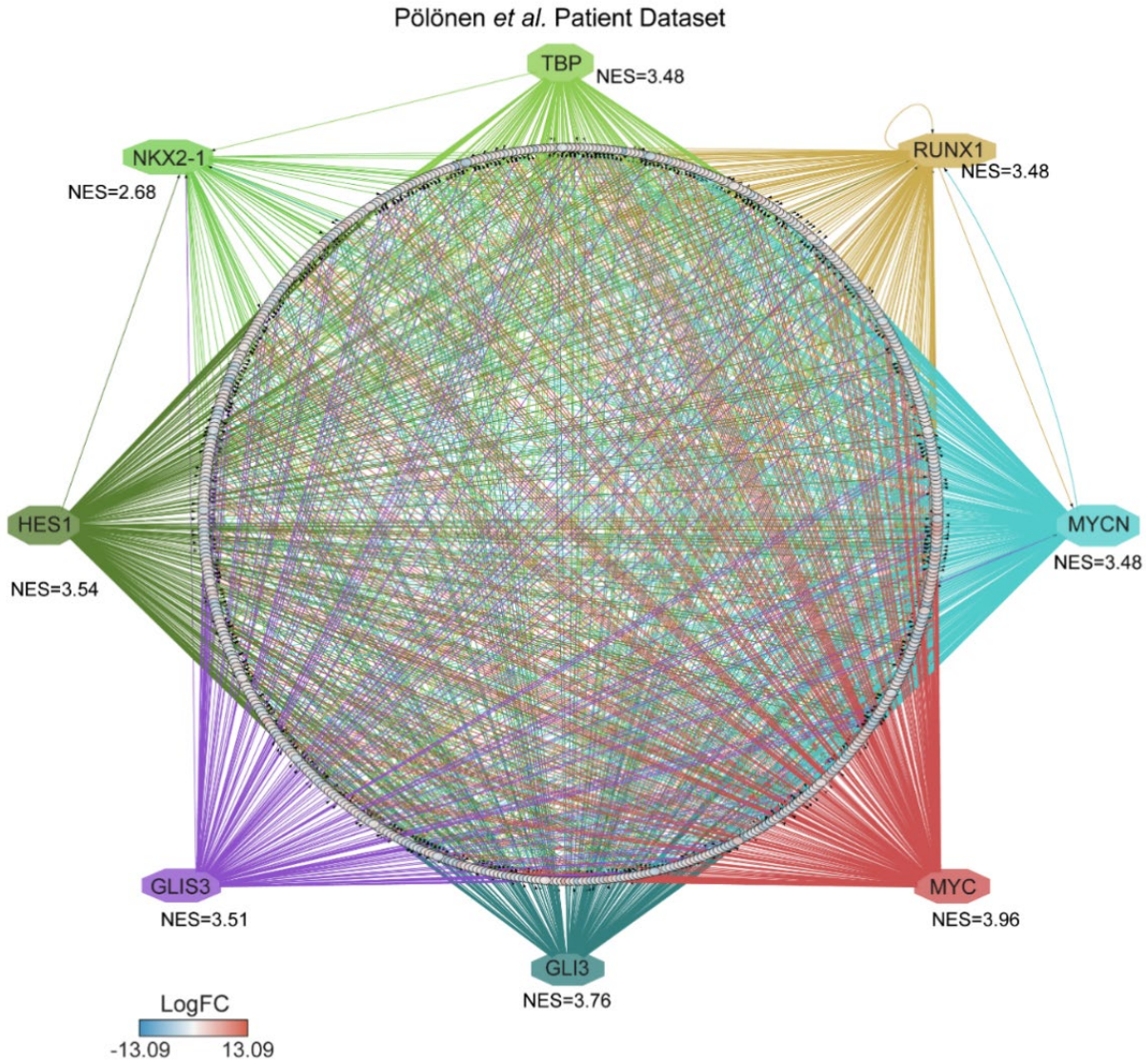

Figure S16. Network representation of transcriptionally regulated genes by NKX2-1 and RUNX1 in public T-ALL RNA-seq patient dataset. iRegulon analysis on top 10% significantly DEGs in NKX2-1 positive versus NKX2-1 negative T-ALL samples. Representative transcription factors from eight top scoring predicted clusters are indicated in the outside octagons. NES values for each cluster code are shown from each transcription factor.

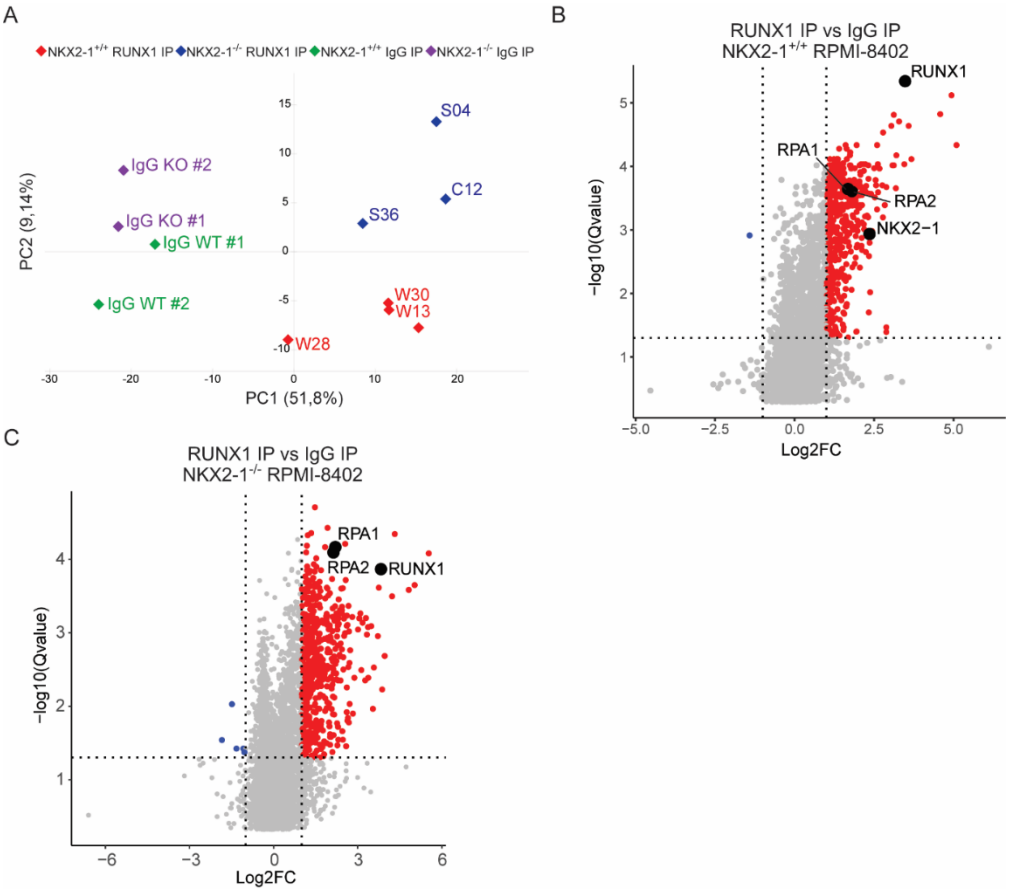

Figure S17. RUNX1 IP-MS in NKX2-1$^{+/+}$ and NKX2-1$^{-/-}$ clones. (A) PCA plot of RUNX1 and IgG IP-MS in NKX2-1$^{+/+}$ and NKX2-1$^{-/-}$ RPMI-8402 clones. **(B-C)** Volcano plot showing differentially detected RUNX1 binding proteins by IP-MS in NKX2-1$^{+/+}$ (B) or NKX2-1$^{-/-}$ (C) compared to IgG of each genotype. The grey-dotted lines indicate the cut-off values for significance (Qvalue<0.05) and fold change (FC>2).

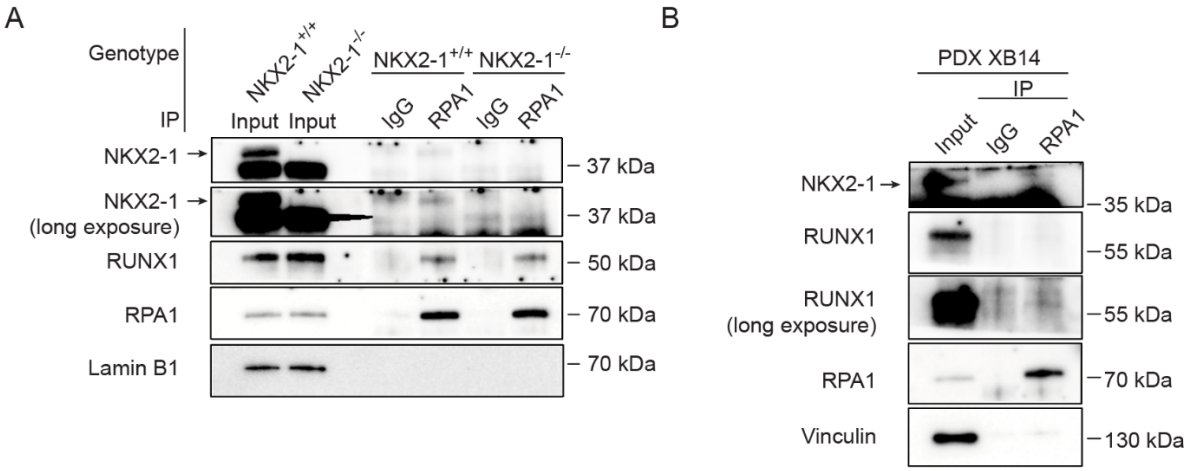

Figure S18. RPA1 co-immunoprecipitates with NKX2-1 and RUNX1 in T-ALL models. (A-B) Immunoblot for NKX2-1, RUNX1 (short and long exposure), RPA1 and Lamin B1 or Vinculin of input, IgG control and NKX2-1 immunoprecipitated samples of NKX2-1$^{+/+}$ or NKX2-1$^{-/-}$ mixed RPMI-8402 clones (A) or NKX2-1-positive PDX XB14 (C).

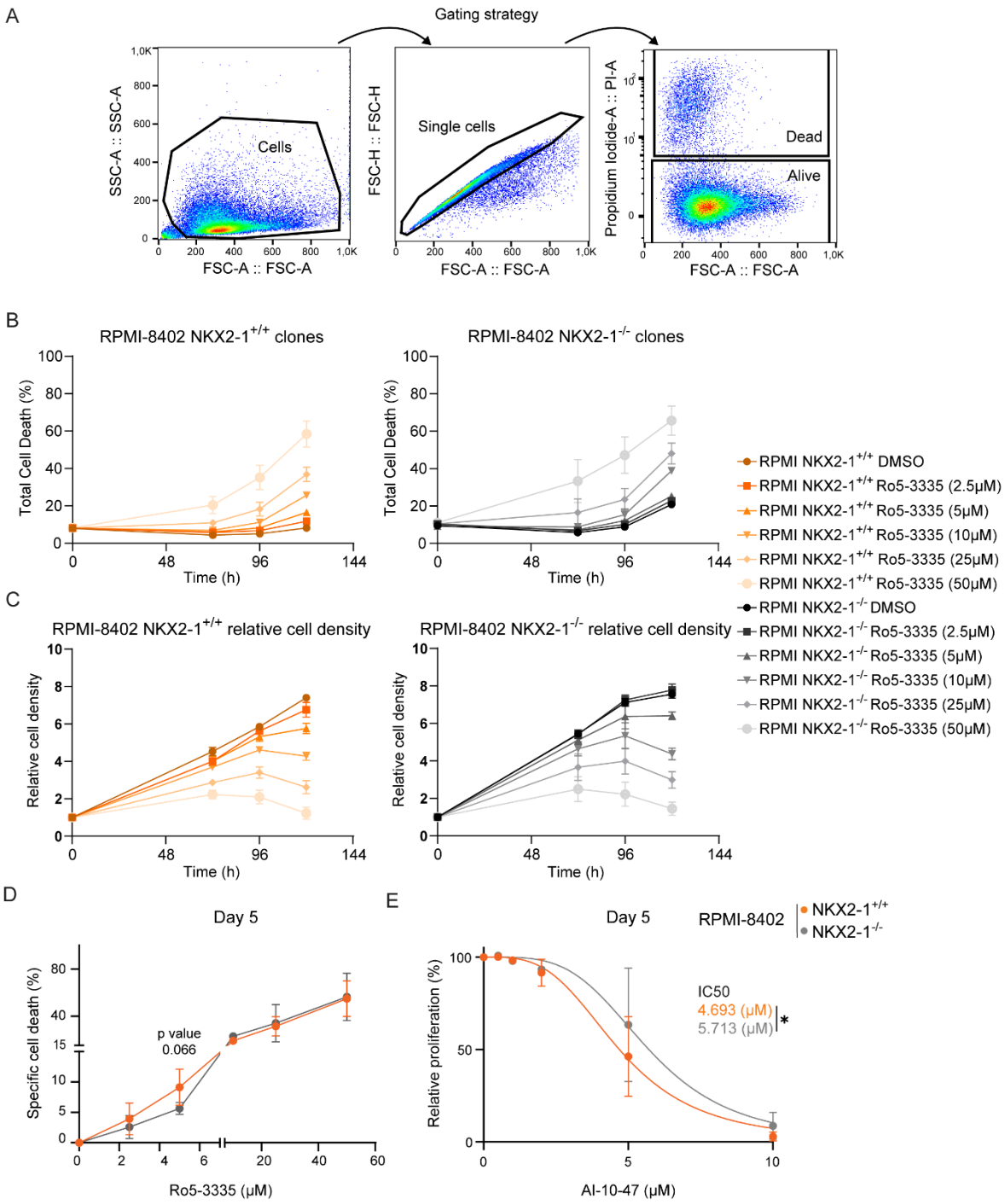

Figure S19. NKX2-1 enhances the sensitivity to pharmacological inhibition of RUNX1 in the RPMI-8402 model. **(A)** Gating strategy for cell viability using PI by flow cytometry. **(B)** Total cell death of NKX2-1$^{+/+}$ and NKX2-1$^{-/-}$ cells after Ro5-3335 treatment for 5 days. Dead cell percentages were determined as PI-positive cells in flow cytometry. **(C)** Proliferation curve of NKX2-1$^{+/+}$ and NKX2-1$^{-/-}$ cells after Ro5-3335 treatment over 5 days. Viable cell numbers plotted are PI-negative staining cells in flow cytometry. **(D)** Specific cell death on NKX2-1$^{+/+}$ and NKX2-1$^{-/-}$ RPMI-8402 cells treated for 5 days with the indicated concentrations of Ro5-3335. Specific cell death calculations were based on PI staining according to the formula specified in the supplementary materials and methods. Data represented as mean ± SD, statistics calculated by an unpaired two-tailed t-test. **(E)** Dose-response curves of NKX2-1$^{+/+}$ and NKX2-1$^{-/-}$ RPMI-8402 clones treated for 120 h with AI-10-47. Data points represent mean ± SD of relative proliferation, normalized to Day 0 and DMSO condition. Least-squares regression fits to the mean are shown (solid lines), and IC50 values were determined for each drug and condition. Statistics were calculated by an extra sum-of-squares F-test. Data in B, C, D and E are represented as

line graphs indicating the average value obtained for four independent clones per genotype, and the error bars indicate the SD on these measurements. *p-value < 0.05.

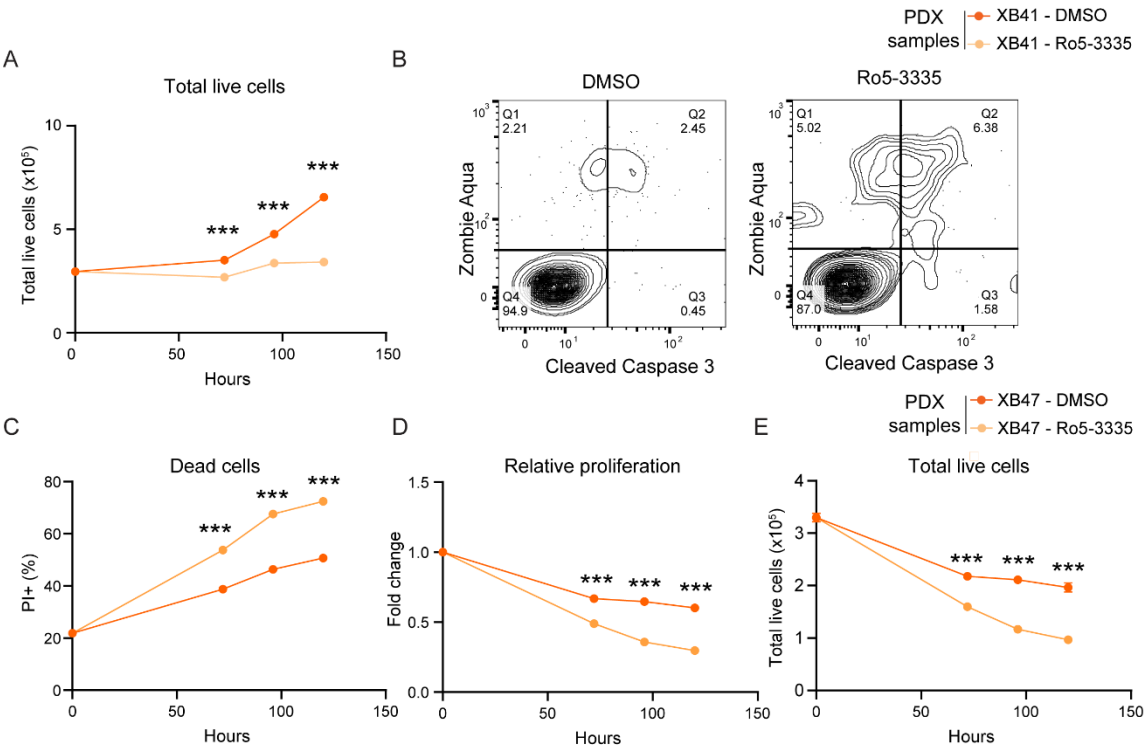

Figure S20. Effect of Ro5-3335 on two *ex vivo* cultured NKX2-1 positive T-ALL PDX samples. Effect of treatment of NKX2-1 positive PDX samples XB41 (top) and XB47 (bottom) with 50 µM Ro5-3335 or DMSO vehicle. **(A)** Total live cells during treatment. **(B)** Flow cytometry analysis of cleaved caspase 3/Zombie Aqua of NKX2-1 positive after 120 h of treatment. **(C)** Relative proliferation of treated XB47 cells normalized to Day 0. **(D)** Absolute percentage of dead cells, identified as PI positive cells by flow cytometry, during treatment. **(E)** Total live cells during treatment. Data in A, C, D and E are represented as mean ± SD of 3 technical replicates, statistics calculated by two-way ANOVA followed by a Šidák test. ***p-value < 0.001.

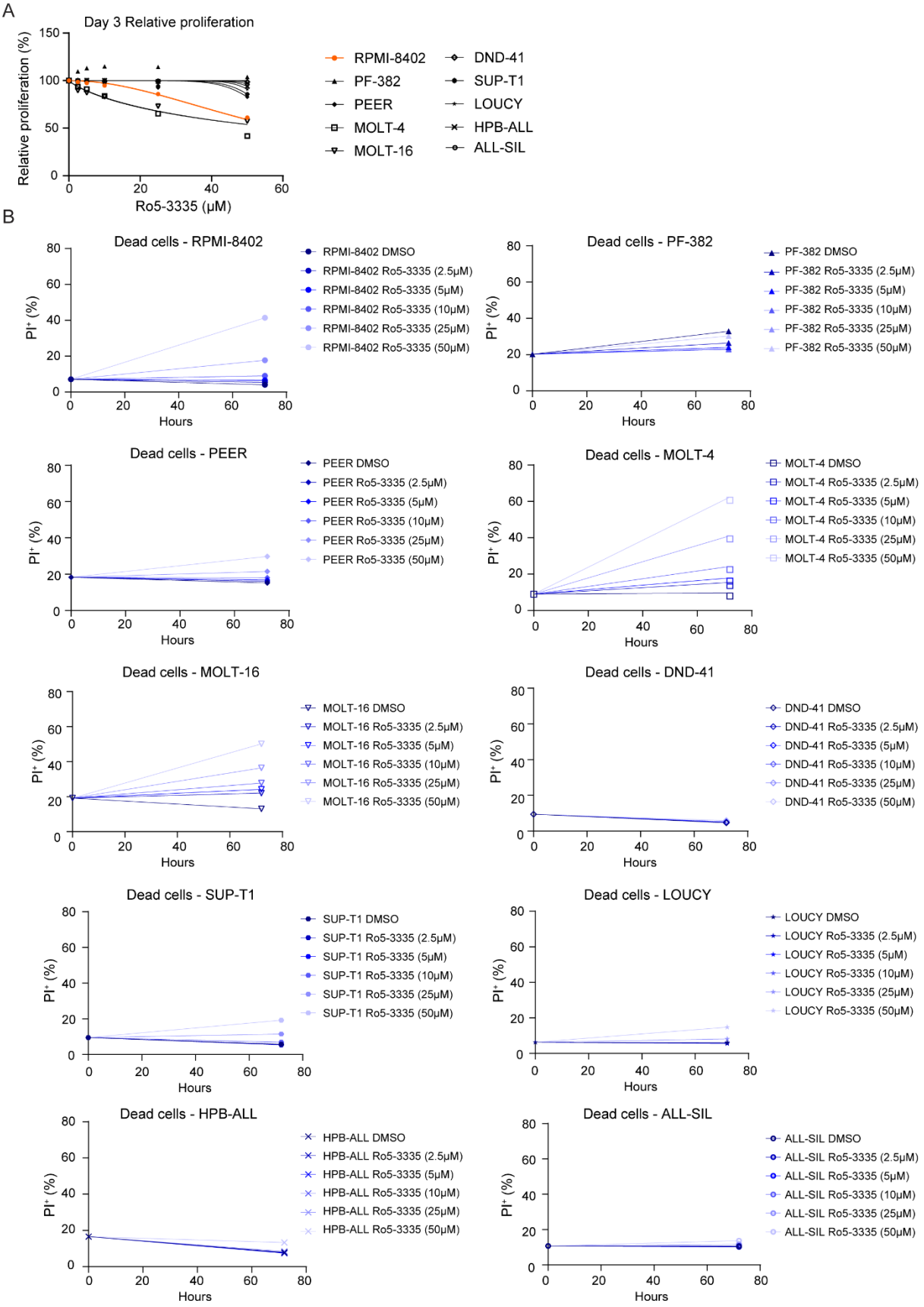

Figure S21. Ro5-3335 response of a panel of human T-ALL cell lines. (A) Dose-response curves of T-ALL cell lines treated for 72 h with Ro5-3335. Data points represent mean ± SD of relative proliferation, normalized to Day 0 and DMSO condition. Least-squares regression fits to the mean are shown (solid lines). The NKX2-1

positive RPMI-8402 cell line was included in the panel and indicated in orange. **(B)** Total cell death of T-ALL cell lines after Ro5-3335 treatment for 72 h. Percentages of dead cells were determined as PI positive cells in flow cytometry.